

Altermagnetic Weyl node-network semimetals protected by spin symmetry

Shuai Qu^{1,2}, Xiao-Yao Hou^{1,2}, Zheng-Xin Liu^{1,2}, Peng-Jie Guo^{1,2,*} and Zhong-Yi Lu^{1,2,3†}

1. School of Physics and Beijing Key Laboratory of Opto-electronic Functional Materials & Micro-nano Devices. Renmin University of China, Beijing 100872, China

2. Key Laboratory of Quantum State Construction and Manipulation (Ministry of Education), Renmin University of China, Beijing 100872, China and

3. Hefei National Laboratory, Hefei 230088, China

(Dated: September 20, 2024)

Symmetry protected topology has been studied extensively in the past twenty years, but the topology protected by spin symmetry has just begun to be studied. In this work, based on spin symmetry analysis, we propose that a class of Weyl nodal line semimetals is protected by the spin symmetry. Then, by the first-principles electronic structure calculations, we predict that both altermagnetic Nb₂FeB₂ and Ta₂FeB₂ are node-network semimetals protected by the spin symmetry. Moreover, both altermagnetic Nb₂FeB₂ and Ta₂FeB₂ have nodal rings protected by the mirror symmetry and Dirac points protected by nonsymmorphic spin symmetry. Furthermore, both altermagnetic Nb₂FeB₂ and Ta₂FeB₂ transform node-network semimetal phase into Weyl semimetal phase when considering spin-orbit coupling. Therefore, our work not only enriches the topological phases protected by spin symmetry, but also provides an excellent material platform to investigate the exotic physical properties of multiple altermagnetic topological semimetal phases in experiment.

Introduction. Symmetry protected topology (SPT) has been studied extensively in condensed matter physics due to rich topological phases and novel physical properties[1–13]. Symmetry plays a pivotal role in the classification of topology and the study of topological properties of materials. Nonmagnetic materials with negligible and strong spin-orbital coupling (SOC) are described by type-II magnetic space groups (MSGs) and their corresponding double groups, respectively. For nonmagnetic materials, the topological classification has been completed by the theories of the symmetry-based indicator and topological chemistry based on band representations, leading to a dictionary of nonmagnetic topological materials[4–10]. On the other hand, the magnetic materials with SOC are described by type-I, II, and IV double MSGs. In consequence, the topological classification has also been completed by the theory of magnetic topological chemistry[11–13]. Moreover, many magnetic topological materials have been extensively studied by theory and experiment, such as MnBi₂Te₄[14].

The magnetic materials with negligible SOC can be described by spin space groups. The spin space groups represent the symmetry transformation of decoupled spin and lattice space. Due to decoupled spin and lattice space, the symmetry transformation of spin and lattice space can be distinct rotation operations. Therefore, conventional MSGs are only subgroups of spin space groups (SSGs). Since the symmetry landscape of SSGs is more plentiful than that of conventional MSGs, there are more novel topological phases protected by spin space symmetry in condensed matter physics. Recently, some topological semimetal and insulator phases protected by spin space group symmetry have been proposed in theory[15–

17]. Moreover, full classification on spin space group has also been completed[18–20]. These works inspire further investigation into the exotic topological phases of spin space symmetry protection.

Recently, based on spin group theory, altermagnetism different from ferromagnetism and antiferromagnetism has been proposed[21, 22]. In altermagnetism, opposite spin sublattices cannot be connected by space-inversion (I) and fractional translation (τ) operations, but only by rotation or mirror (R) operations. Correspondingly, altermagnetic materials break the spin symmetry $\{C_2^\perp||I\}$ and $\{C_2^\perp||\tau\}$, but have the spin symmetry $\{C_2^\perp||R\}$ (the C_2^\perp represents 180 degrees rotation perpendicular to the spin direction). The breaking of the spin symmetries $\{C_2^\perp||I\}$ and $\{C_2^\perp||\tau\}$ result in the spin splitting, while the spin symmetry $\{C_2^\perp||R\}$ guarantees the total magnetic moment to be zero. Therefore, altermagnetism has the duality of real-space antiferromagnetism and momentum-space anisotropic spin splitting. On the other hand, under spin-orbit coupling, the symmetry of altermagnetic materials will change from spin group symmetry to magnetic group symmetry. In particular, the spin symmetries $\{C_2^\perp||I\}$ and $\{C_2^\perp||\tau\}$ will change to IT and $T\tau$ symmetries (equivalent time-reversal symmetry), respectively, so that the altermagnetic materials break the equivalent time-reversal symmetry. Due to the duality of real-space antiferromagnetism and momentum-space anisotropic spin splitting and the breaking of equivalent time-reversal symmetry under spin-orbit coupling, altermagnetic materials have many novel physical properties[23–48]. Therefore, altermagnetic materials may be an excellent platform for exploring novel topological phases.

In this work, based on spin symmetry analysis, we propose a new Weyl nodal line protected by the spin space symmetry $\{TC_2^\perp||IT\}$. Then, by the first-principles electronic structure calculations, we predict that both

* guopengjie@ruc.edu.cn

† zlu@ruc.edu.cn

altermagnetic Nb_2FeB_2 and Ta_2FeB_2 are Weyl node-network semimetals protected by the spin symmetry $\{\text{TC}_2^\perp \parallel \text{IT}\}$. Moreover, both Nb_2FeB_2 and Ta_2FeB_2 also have Weyl nodal lines protected by the mirror symmetry and 16 Dirac points protected by nonsymmorphic spin symmetry. When considering SOC, both altermagnetic Nb_2FeB_2 and Ta_2FeB_2 will transform the node-network semimetal phase into the Weyl semimetal phase.

Method The first-principles electronic structure calculations were performed in the framework of density functional theory (DFT) using the Vienna Abinitio Simulation Package (VASP)[49–53]. The generalized gradient approximation (GGA) of Perdew–Burke–Ernzerhof (PBE) type was adopted for the exchange correlation functional[54]. The projector augmented wave (PAW) method was adopted to describe the interactions between valence electrons and nuclei[55, 56]. The kinetic energy cutoff of the plane-wave basis was set to be 600eV. The total energy convergence and the atomic force tolerance were set to be 10^{-6} eV and 0.01eV/Å, respectively. For describing the Fermi-Dirac distribution function, a Gaussian smearing of 0.05eV was used. An $8 \times 8 \times 15$ k-point mesh was used for the Brillouin Zone (BZ) sampling. To account for the correlation effects of Fe $3d$ orbitals, we performed GGA + U calculations by using the simplified rotationally invariant version of Dudarev et al[57, 58]. By the linear response method[59], the on-site effective U_{eff} values of Fe d -electron of Nb_2FeB_2 and Ta_2FeB_2 were estimated to be 4.82eV and 4.76eV, respectively, which were used to study electronic structures of Nb_2FeB_2 and Ta_2FeB_2 . The topological properties of Nb_2FeB_2 and Ta_2FeB_2 were calculated by `wannier90`[60–62] and `Wanniertools`[63] software packages.

Symmetry analysis In two-dimensional systems, the spin symmetry $\{\text{TC}_2^\perp \parallel \text{IT}\}$ can quantize the berry curvature $\Omega(\mathbf{k})$ to 0 or π and the Berry curvature $\Omega(\mathbf{k})=\pi$ corresponds a Weyl point at \mathbf{k} point[35]. That is to say, the spin symmetry $\{\text{TC}_2^\perp \parallel \text{IT}\}$ can protect Weyl points at general \mathbf{k} points in the two-dimensional BZ[35]. If generalizing two-dimensional systems to three-dimensional systems, the spin space symmetry $\{\text{TC}_2^\perp \parallel \text{IT}\}$ can naturally protect three-dimensional Weyl node-line semimetals. Moreover, the Weyl nodal line can be located in any region of BZ, which is similar to the Dirac nodal line protected by IT symmetry in nonmagnetic materials. Then, a natural question is what materials may be Weyl node-line semimetals protected by the spin space symmetry $\{\text{TC}_2^\perp \parallel \text{IT}\}$. First, the electronic bands of these materials have spin-splitting in the nonrelativistic case. Second, these materials have the spin space symmetry $\{\text{TC}_2^\perp \parallel \text{IT}\}$ and the corresponding electronic structures have band crossing.

Results Very recently, Nb_2FeB_2 and Ta_2FeB_2 have been predicted to be \mathbf{g} -wave altermagnetic materials with large intrinsic anomalous Hall effects (AHE)[33, 42]. The crystal structures of Nb_2FeB_2 and Ta_2FeB_2 are illustrated in Fig. 1(a). From the Fig. 1(a), the crystal primitive cell contains two formula units and is com-

posed of Fe – B and Nb(Ta) atomic layers. The magnetic primitive cell is the same as the crystal primitive cell (Fig. 1(a)) and the corresponding bulk BZ and projected two-dimensional surface BZ are illustrated in Fig. 1(b). In the nonrelativistic case, the symmetry of altermagnetic Nb_2FeB_2 and Ta_2FeB_2 are described by spin group and the corresponding generators are $\{\text{TC}_2^\perp \parallel \text{T}\}$, $\{\text{E} \parallel \text{I}\}$, $\{\text{C}_2^\perp \parallel \text{C}_{2x}(1/2, 1/2)\}$, $\{\text{E} \parallel \text{C}_{2z}\}$, $\{\text{E} \parallel \text{C}_{4z}\}$. Therefore, both Nb_2FeB_2 and Ta_2FeB_2 have the spin symmetry $\{\text{TC}_2^\perp \parallel \text{IT}\}$.

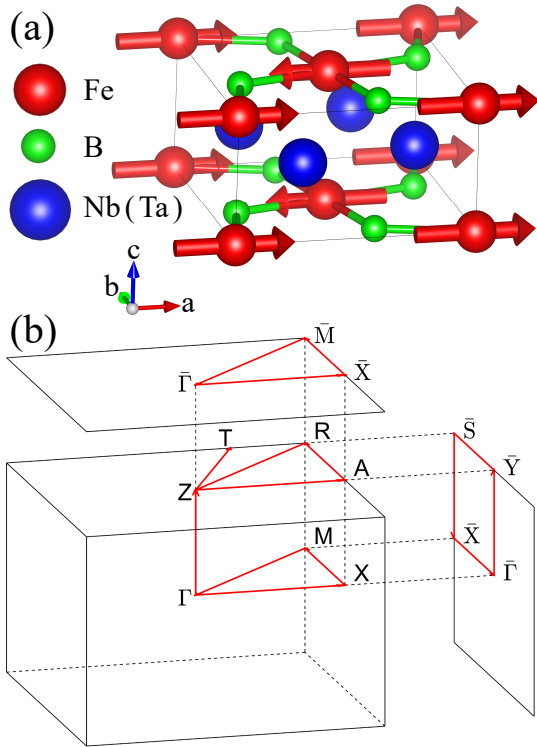


FIG. 1. (a) Crystal structures of the Nb_2FeB_2 and Ta_2FeB_2 . The red arrows indicate magnetic momentum. (b) The corresponding bulk BZ and projected two-dimensional surface BZ. The red lines represent the high-symmetry paths.

Now we study the electronic structures of altermagnetic Nb_2FeB_2 and Ta_2FeB_2 . Since altermagnetic Nb_2FeB_2 and Ta_2FeB_2 have the similar electronic structures, we only show the results of Nb_2FeB_2 in the following. The calculated electronic band structures of altermagnetic Nb_2FeB_2 without SOC are shown in Fig. 2(a). From Fig. 2(a), Nb_2FeB_2 is an altermagnetic semimetal. Due to the absence of the spin symmetries $\{\text{C}_2^\perp \parallel \text{I}\}$ and $\{\text{C}_2^\perp \parallel \tau\}$, spin-up and spin-down bands should be split in the Nb_2FeB_2 . However, these bands of Nb_2FeB_2 along the high-symmetry directions are always degeneracy. By symmetry analysis, we find that the spin degeneracy along the high-symmetry direction is protected by these spin symmetries $\{\text{C}_2^\perp \parallel \text{C}_{2x}(1/2, 1/2)\}$, $\{\text{C}_2^\perp \parallel \text{C}_{2y}(1/2, 1/2)\}$, $\{\text{C}_2^\perp \parallel \text{C}_{xy}(1/2, 1/2)\}$, and $\{\text{C}_2^\perp \parallel \text{C}_{x-y}(1/2, 1/2)\}$. To demonstrate the anisotropic spin splitting caused by al-

ternating magnetism, we also calculate the band structures of Nb_2FeB_2 along the non-high-symmetry Z-T direction. Indeed, these bands along the non-high-symmetry Z-T direction are spin-splitting reflecting the characteristics of g -wave splitting (Fig. 2(a)).

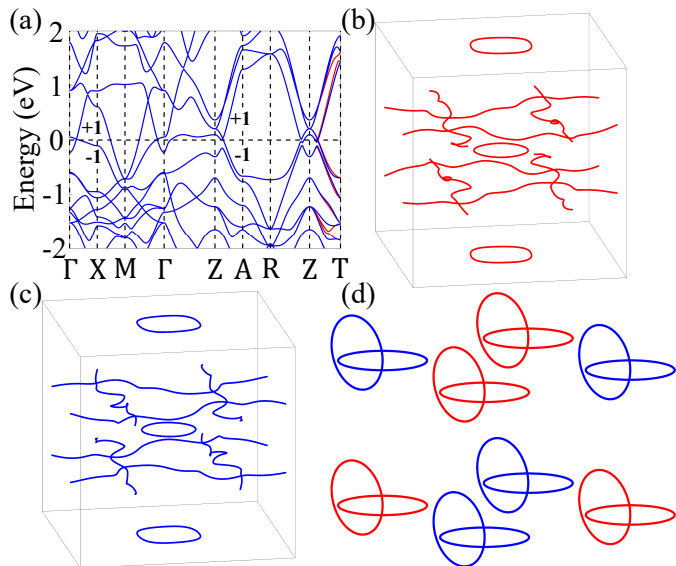


FIG. 2. (a) The spin-resolved electronic band structures of Nb_2FeB_2 without SOC along the high-symmetry and non-high-symmetry directions. (b) and (c) are nodal structures of spin-up and spin-down bands, respectively. (d) Hopf-link nodal lines protected by the spin symmetry $\{TC_2^{\perp}||IT\}$. The red and blue represent the spin-up and spin-down bands, respectively. The 1 and -1 are the eigenvalues of the mirror $\{E||M_z\}$ of the two crossing bands around the Fermi level.

Interestingly, altermagnetic Nb_2FeB_2 has multiple crossing points around the Fermi level, which implies altermagnetism with nontrivial topological properties. These crossing points on the $\Gamma - X$, $\Gamma - M$, $Z - A$, $Z - R$, and $Z - T$ axes indicate that altermagnetic Nb_2FeB_2 may have two Weyl nodal rings protected by the mirror symmetry $\{E||M_z\}$ on $k_z = 0$ and π planes around the Fermi level for spin-up or spin-down bands (Fig. 2(a)). To confirm it, we calculate nodes of two crossing spin-up (spin-down) bands around the Fermi level in the whole BZ, which are shown in Fig. 2(b) and (c). Obviously, there are two Weyl nodal rings on the $k_z = 0$ and π planes for spin-up (spin-down) bands. Since the two crossing bands with opposite eigenvalues of mirror $\{E||M_z\}$ (Fig. 2(a)), the two Weyl nodal rings on the $k_z = 0$ and π planes are protected by the mirror symmetry $\{E||M_z\}$. On the other hand, due to the spin degeneracy along the high-symmetry directions, all crossing points on the $\Gamma - X$, $\Gamma - M$, $Z - A$, and $Z - R$ are fourfold degenerate Dirac points. Considering the $\{E||C_{4z}\}$ spin symmetry, altermagnetic Nb_2FeB_2 has 16 Dirac points.

More significantly, in addition to the two Weyl nodal rings on the $k_z = 0$ and π planes, there are two Weyl nodal networks between $k_z = 0$ and π for spin-up (Fig.

2(b)) or spin-down (Fig. 2(c)) bands. Since locating at general area in the BZ, the two Weyl nodal networks are only protected by the spin symmetry $\{TC_2^{\perp}||IT\}$. As far as we know, the class of new Weyl nodal line semimetal is proposed for the first time. Moreover, the Weyl nodal network consists of four nodal lines and the four nodal lines don't intersect with each other. Due to periodic boundary condition, a Weyl nodal network can form two Hopf-link Weyl nodal lines (Fig. 2(d))[64]. Therefore, there are eight Hopf-link Weyl nodal lines for both spin-up and spin-down bands (Fig. 2(d)).

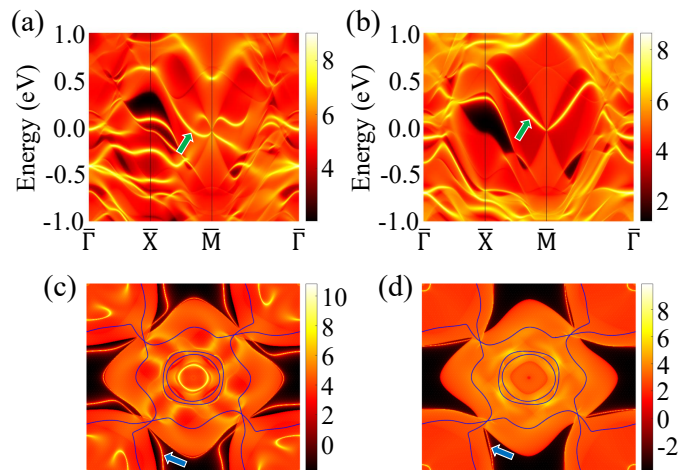


FIG. 3. Spectral function of unconventional collinear AFM Nb_2FeB_2 along the high-symmetry directions in the projected 2D BZ of the (001) surface with left (a) and right (b) semi-infinite termination boundaries for the spin-up bands. The spectral function at the Fermi level with left (c) and right (d) semi-infinite termination boundaries. The blue lines represent nodal lines.

As well-known to all, nontrivial node-line semimetals have topological protected drumhead surface states. Since these Weyl nodal networks and rings can be projected to the (001) surface, altermagnetic Nb_2FeB_2 has also nontrivial surface states, which are confirmed by the calculated spectral function of the (001) surface with semi-infinite termination boundary. Since spin-up and spin-down electronic structures have similar topological surface states, we only show these results for spin-up electronic structures. From the Fig. 3(a) and (b), there are nontrivial drumhead surface states derived from the nodal ring protected by mirror symmetry, which are marked by green arrows. Interestingly, the nodal networks protected by the spin symmetry $\{TC_2^{\perp}||IT\}$ also have nontrivial surface states which are marked by blue arrows (Fig. 3(c) and (d)).

With SOC, due to coupled spin and lattice space, the symmetry transformation of spin and lattice space must be the same symmetry operation. Correspondingly, the symmetry of altermagnetic Nb_2FeB_2 changes from spin point group to magnetic point group. Moreover, the magnetic point group symmetry depends on the direction of

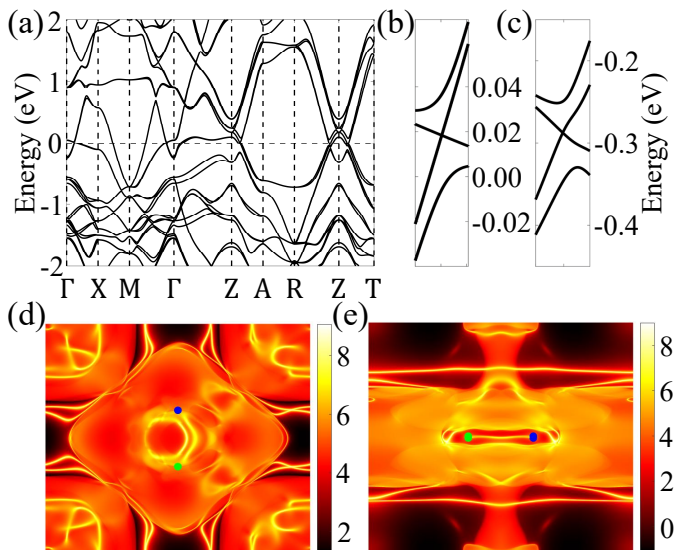


FIG. 4. (a) The electronic band structures of unconventional collinear AFM Nb_2FeB_2 with SOC along the high-symmetry and non-high-symmetry directions. (b) and (c) represent Weyl points above and under the Fermi level, respectively. The spectral function at the energy of Weyl points with semi-infinite termination at the (d) (001) and (e) (100) boundaries. The green and blue dots represent Weyl points with topological charge 1 and -1, respectively.

the easy magnetization axis. Since the easy magnetization axis of altermagnetic Nb_2FeB_2 is along the x direction [33], altermagnetic Nb_2FeB_2 has $C_{2y}(1/2, 1/2)$, I , $M_y(1/2, 1/2)$, $C_{2x}(1/2, 1/2)T$, $M_x(1/2, 1/2)T$, $C_{2z}T$, M_zT symmetries. Then, we calculate the electronic band structures of altermagnetic Nb_2FeB_2 with SOC, which are illustrated in Fig. 4 (a). Since the spin symmetries $\{E||M_z\}$ and $\{TC_2^\perp||IT\}$ are broken, these Weyl nodal rings and networks open gap, but the bandgap is very small due to the weak SOC (Fig. 4 (a)). This is advantageous for having an opportunity to manipulate the novel properties of nodal networks protected by the spin symmetry $\{TC_2^\perp||IT\}$ in experiment.

In general, Weyl node-line semimetals transform into Weyl semimetals when considering SOC. Our calculations also show that altermagnetic Nb_2FeB_2 indeed transforms into a Weyl semimetal and has 84 Weyl points. According to magnetic symmetry analysis, there are only 12 independent Weyl points, which are shown in Table I. Then, we calculate the two Weyl points closest to the Fermi level for altermagnetic Nb_2FeB_2 which are shown in Fig. 4 (b) and (c). From Fig. 4 (b) and (c), altermagnetic Nb_2FeB_2 is type-I Weyl semimetal. In order to

display the characteristics of Weyl semimetal more intuitively, we also calculate the chirality of all Weyl points (Table I) and topological protected Fermi arc (Fig. 4 (d) and (e)). From Fig. 4 (d) and (e), topological protected Fermi arc connects the two Weyl points with opposite chirality. Thus, Nb_2FeB_2 is an altermagnetic Weyl semi-

TABLE I. The position and chirality of 12 independent Weyl points in altermagnetic Nb_2FeB_2

Position	Chirality
(0.492, 0.484, 0.041)	-1.000
(0.259, 0.445, 0.148)	-1.000
(0.391, 0.270, 0.137)	1.000
(0.467, 0.252, 0.156)	-1.000
(0.000, 0.123, 0.004)	-1.000
(0.181, 0.222, 0.117)	1.000
(0.213, 0.123, 0.159)	-1.000
(0.118, 0.213, 0.157)	1.000
(0.215, 0.109, 0.150)	1.000
(0.000, 0.280, 0.127)	-1.000
(0.271, 0.021, 0.124)	-1.000
(0.000, 0.259, 0.121)	-1.000

metal under SOC. Finally, our calculations show that Ta_2FeB_2 and Nb_2FeB_2 have the same topological properties.

In summary, based on the symmetry analysis, we propose a new type of Weyl node-line semimetal protected by the spin symmetry $\{TC_2^\perp||IT\}$. Then, by the first-principles electronic structure calculations, we predict that altermagnetic Nb_2FeB_2 is node-network semimetal protected by the spin symmetry $\{TC_2^\perp||IT\}$. Moreover, altermagnetic Nb_2FeB_2 will transform the node-network semimetal phase into the Weyl semimetal phase when considering SOC. Our study not only enriches the topology class protected by the spin space symmetry, but also provides an excellent platform to explore the exotic physical properties of node-network semimetals protected by the spin space symmetry.

ACKNOWLEDGMENTS

This work was financially supported by the National Natural Science Foundation of China (Grants No.11934020 and No.12204533) and the Fundamental Research Funds for the Central Universities, and the Research Funds of Renmin University of China (Grant No. 24XNKJ15). Computational resources have been provided by the Physical Laboratory of High Performance Computing at Renmin University of China.

- [1] M. Z. Hasan and C. L. Kane, Colloquium: Topological insulators, *Rev. Mod. Phys.* **82**, 3045 (2010).
 [2] X.-L. Qi and S.-C. Zhang, Topological insulators and su-

- perconductors, *Rev. Mod. Phys.* **83**, 1057 (2011).
 [3] H. Weng, X. Dai, and Z. Fang, Topological semimetals predicted from first-principles calculations, *J. Phys.:*

- Condens.Matter **28**, 303001 (2016).
- [4] B. Bradlyn, L. Elcoro, J. Cano, M. G. Vergniory, Z. Wang, C. Felser, M. I. Aroyo, and B. A. Bernevig, Topological quantum chemistry, *Nature* **547**, 298 (2017).
- [5] H. C. Po, A. Vishwanath, and H. Watanabe, Symmetry-based indicators of band topology in the 230 space groups, *Nat. Commun.* **8**, 50 (2017).
- [6] Z. Song, T. Zhang, Z. Fang, and C. Fang, Quantitative mappings between symmetry and topology in solids, *Nat. Commun.* **9**, 3530 (2018).
- [7] F. Tang, H. C. Po, A. Vishwanath, and X. Wan, Efficient topological materials discovery using symmetry indicators, *Nat. Phys.* **15**, 470 (2019).
- [8] F. Tang, H. C. Po, A. Vishwanath, and X. Wan, Comprehensive search for topological materials using symmetry indicators, *Nature* **566**, 486 (2019).
- [9] M. G. Vergniory, L. Elcoro, C. Felser, N. Regnault, B. A. Bernevig, and Z. Wang, A complete catalogue of high-quality topological materials, *Nature* **566**, 480 (2019).
- [10] T. Zhang, Y. Jiang, Z. Song, H. Huang, Y. He, Z. Fang, H. Weng, and C. Fang, Catalogue of topological electronic materials, *Nature* **566**, 475 (2019).
- [11] Y. Xu, L. Elcoro, Z. Song, B. J. Wieder, M. G. Vergniory, N. Regnault, Y. Chen, C. Felser, and B. A. Bernevig, High-throughput calculations of magnetic topological materials, *Nature* **586**, 702 (2020).
- [12] L. Elcoro, B. J. Wieder, Z. Song, Y. Xu, and B. A. Bernevig, Magnetic topological quantum chemistry, *Nat. Commun.* **12**, 5965 (2021).
- [13] B. Peng, Y. Jiang, Z. Fang, H. Weng, and C. Fang, Topological classification and diagnosis in magnetically ordered electronic materials, *Phys. Rev. B* **105**, 235138 (2022).
- [14] M. M. Otrokov, I. I. Klimovskikh, H. Bentmann, D. Estyunin, A. Zeugner, Z. S. Aliev, S. Gaß, A. U. B. Wolter, A. V. Koroleva, A. M. Shikin, M. Blanco-Rey, M. Hoffmann, I. P. Rusinov, A. Y. Vyazovskaya, S. V. Eremeev, Y. M. Koroteev, V. M. Kuznetsov, F. Freyse, J. Sánchez-Barriga, I. R. Amiraslanov, M. B. Babanly, N. T. Mamedov, N. A. Abdullayev, V. N. Zverev, V. N. Zverev, A. Alfonsov, V. Kataev, B. Büchner, E. F. Schwier, S. Kumar, A. Kimura, L. Petaccia, G. Di Santo, R. C. Vidal, S. Schatz, K. Kißner, M. Ünzelmann, C. H. Min, S. Moser, T. R. F. Peixoto, T. R. F. Peixoto, F. Reinert, A. Ernst, P. M. Echenique, A. Isaeva, and E. V. Chulkov, Prediction and observation of an antiferromagnetic topological insulator, *Nature* **576**, 416 (2019).
- [15] P.-J. Guo, Y.-W. Wei, K. Liu, Z.-X. Liu, and Z.-Y. Lu, Eightfold degenerate fermions in two dimensions, *Phys. Rev. Lett.* **127**, 176401 (2021).
- [16] P. Liu, J. Li, J. Han, X. Wan, and Q. Liu, Spin-group symmetry in magnetic materials with negligible spin-orbit coupling, *Phys. Rev. X* **12**, 021016 (2022).
- [17] P. Liu, A. Zhang, J. Han, and Q. Liu, Chiral dirac-like fermion in spin-orbit-free antiferromagnetic semimetals, *The Innovation* **3**, 100343 (2022).
- [18] X. Chen, J. Ren, Y. Zhu, Y. Yu, A. Zhang, P. Liu, J. Li, Y. Liu, C. Li, and Q. Liu, Enumeration and representation theory of spin space groups, *Phys. Rev. X* **14**, 031038 (2024).
- [19] Y. Jiang, Z. Song, T. Zhu, Z. Fang, H. Weng, Z.-X. Liu, J. Yang, and C. Fang, Enumeration of spin-space groups: Toward a complete description of symmetries of magnetic orders, *Phys. Rev. X* **14**, 031039 (2024).
- [20] Z. Xiao, J. Zhao, Y. Li, R. Shindou, and Z.-D. Song, Spin space groups: Full classification and applications, *Phys. Rev. X* **14**, 031037 (2024).
- [21] L. Šmejkal, J. Sinova, and T. Jungwirth, Emerging Research Landscape of Altermagnetism, *Phys. Rev. X* **12**, 040501 (2022).
- [22] L. Šmejkal, J. Sinova, and T. Jungwirth, Beyond Conventional Ferromagnetism and Antiferromagnetism: A Phase with Nonrelativistic Spin and Crystal Rotation Symmetry, *Phys. Rev. X* **12**, 031042 (2022).
- [23] I. Mazin, Editorial: Altermagnetism—a new punch line of fundamental magnetism, *Phys. Rev. X* **12**, 040002 (2022).
- [24] R. González-Hernández, L. Šmejkal, K. Výborný, Y. Yahagi, J. Sinova, T. Jungwirth, and J. Železný, Efficient Electrical Spin Splitter Based on Nonrelativistic Collinear Antiferromagnetism, *Phys. Rev. Lett.* **126**, 127701 (2021).
- [25] H. Bai, L. Han, X. Y. Feng, Y. J. Zhou, R. X. Su, Q. Wang, L. Y. Liao, W. X. Zhu, X. Z. Chen, F. Pan, X. L. Fan, and C. Song, Observation of Spin Splitting Torque in a Collinear Antiferromagnet RuO₂, *Phys. Rev. Lett.* **128**, 197202 (2022).
- [26] A. Bose, N. J. Schreiber, R. Jain, D.-F. Shao, H. P. Nair, J. Sun, X. S. Zhang, D. A. Muller, E. Y. Tsymbal, D. G. Schlom, and D. C. Ralph, Tilted spin current generated by the collinear antiferromagnet ruthenium dioxide, *Nat. Electron.* **5**, 267 (2022).
- [27] S. Karube, T. Tanaka, D. Sugawara, N. Kadoguchi, M. Kohda, and J. Nitta, Observation of Spin-Splitter Torque in Collinear Antiferromagnetic RuO₂, *Phys. Rev. Lett.* **129**, 137201 (2022).
- [28] L. Šmejkal, A. B. Hellenes, R. González-Hernández, J. Sinova, and T. Jungwirth, Giant and Tunneling Magnetoresistance in Unconventional Collinear Antiferromagnets with Nonrelativistic Spin-Momentum Coupling, *Phys. Rev. X* **12**, 011028 (2022).
- [29] D.-F. Shao, S.-H. Zhang, M. Li, C.-B. Eom, and E. Tsymbal, Spin-neutral currents for spintronics, *Nat. Commun.* **12**, 7061 (2021).
- [30] H.-Y. Ma, M. Hu, N. Li, J. Liu, W. Yao, J.-F. Jia, and J. Liu, Multifunctional antiferromagnetic materials with giant piezomagnetism and noncollinear spin current, *Nat. Commun.* **12**, 2846 (2021).
- [31] L. Šmejkal, A. H. MacDonald, J. Sinova, S. Nakatsuji, and T. Jungwirth, Anomalous Hall antiferromagnets, *Nat. Rev. Mater.* **7**, 482 (2022).
- [32] Z. Feng, X. Zhou, L. Šmejkal, L. Wu, Z. Zhu, H. Guo, R. González-Hernández, X. Wang, H. Yan, P. Qin, X. Zhang, H. Wu, H. Chen, Z. Meng, L. Liu, Z. Xia, J. Sinova, T. Jungwirth, and Z. Liu, An anomalous hall effect in altermagnetic ruthenium dioxide, *Nat. Electron.* **5**, 735 (2022).
- [33] X.-Y. Hou, H.-C. Yang, Z.-X. Liu, P.-J. Guo, and Z.-Y. Lu, Large intrinsic anomalous Hall effect in both Nb₂FeB₂ and Ta₂FeB₂ with collinear antiferromagnetism, *Phys. Rev. B* **107**, L161109 (2023).
- [34] R. D. Gonzalez Betancourt, J. Zubáč, R. Gonzalez-Hernandez, K. Geishendorf, Z. Šobáň, G. Springholz, K. Olejník, L. Šmejkal, J. Sinova, T. Jungwirth, S. T. B. Goennenwein, A. Thomas, H. Reichlová, J. Železný, and D. Kriegner, Spontaneous Anomalous Hall Effect Arising from an Unconventional Compensated Magnetic Phase in a Semiconductor, *Phys. Rev. Lett.* **130**, 036702 (2023).

- [35] P.-J. Guo, Z.-X. Liu, and Z.-Y. Lu, Quantum anomalous hall effect in collinear antiferromagnetism, *npj Comput. Mater.* **9**, 70 (2023).
- [36] D. Zhu, Z.-Y. Zhuang, Z. Wu, and Z. Yan, Topological superconductivity in two-dimensional altermagnetic metals, *Phys. Rev. B* **108**, 184505 (2023).
- [37] X. Zhou, W. Feng, R.-W. Zhang, L. Šmejkal, J. Sinova, Y. Mokrousov, and Y. Yao, Crystal Thermal Transport in Altermagnetic RuO₂, *Phys. Rev. Lett.* **132**, 056701 (2024).
- [38] P.-J. Guo, Y. Gu, Z.-F. Gao, and Z.-Y. Lu, Altermagnetic ferroelectric LiFe₂F₆ and spin-triplet excitonic insulator phase (2023), arXiv:2312.13911 [cond-mat.mtrl-sci].
- [39] S. Qu, Z.-F. Gao, H. Sun, K. Liu, P.-J. Guo, and Z.-Y. Lu, Extremely strong spin-orbit coupling effect in light element altermagnetic materials (2024), arXiv:2401.11065 [cond-mat.mtrl-sci].
- [40] Y.-X. Li and C.-C. Liu, Majorana corner modes and tunable patterns in an altermagnet heterostructure, *Phys. Rev. B* **108**, 205410 (2023).
- [41] Y.-X. Li, Y. Liu, and C.-C. Liu, Creation and manipulation of higher-order topological states by altermagnets, *Phys. Rev. B* **109**, L201109 (2024).
- [42] Z.-F. Gao, S. Qu, B. Zeng, Y. Liu, J.-R. Wen, H. Sun, P.-J. Guo, and Z.-Y. Lu, AI-accelerated Discovery of Altermagnetic Materials (2023), arXiv:2311.04418 [cond-mat.mes-hall].
- [43] S. Zeng and Y.-J. Zhao, Description of two-dimensional altermagnetism: Categorization using spin group theory, *Phys. Rev. B* **110** (2024).
- [44] J. Krempaský, L. Šmejkal, S. W. D'Souza, M. Hajlaoui, G. Springholz, K. Uhlířová, F. Alarab, P. C. Constantinou, V. Strocov, D. Usanov, W. R. Pudelko, R. González-Hernández, A. B. Hellenes, Z. Jansa, H. Reichlová, Z. Šobáň, R. D. G. Betancourt, P. Wadley, J. Sinova, D. Kriegner, J. Minár, J. H. Dil, and T. Jungwirth, Altermagnetic lifting of Kramers spin degeneracy, *Nature* **626**, 517 (2024).
- [45] Y. Liu, J. Yu, and C.-C. Liu, Twisted Magnetic Van der Waals Bilayers: An Ideal Platform for Altermagnetism (2024), arXiv:2404.17146 [cond-mat.mtrl-sci].
- [46] S. Reimers, L. Odenbreit, L. Šmejkal, V. N. Strocov, P. Constantinou, A. B. Hellenes, R. J. Ubierno, W. H. Campos, V. K. Bharadwaj, A. Chakraborty, T. Deneulin, W. Shi, R. E. Dunin-Borkowski, S. Das, M. Kläui, J. Sinova, and M. Jourdan, Direct observation of altermagnetic band splitting in CrSb thin films, *Nat. Commun.* **15**, 2116 (2024).
- [47] T. Osumi, S. Souma, T. Aoyama, K. Yamauchi, A. Honma, K. Nakayama, T. Takahashi, K. Ohgushi, and T. Sato, Observation of a giant band splitting in altermagnetic MnTe, *Phys. Rev. B* **109**, 115102 (2024).
- [48] C.-Y. Tan, Z.-F. Gao, H.-C. Yang, K. Liu, P.-J. Guo, and Z.-Y. Lu, Bipolarized Weyl semimetals and quantum crystal valley Hall effect in two-dimensional altermagnetic materials (2024), arXiv:2406.16603 [cond-mat.mtrl-sci].
- [49] P. Hohenberg and W. Kohn, Inhomogeneous electron gas, *Phys. Rev.* **136**, B864 (1964).
- [50] W. Kohn and L. J. Sham, Self-consistent equations including exchange and correlation effects, *Phys. Rev.* **140**, A1133 (1965).
- [51] G. Kresse and J. Furthmüller, Efficiency of ab-initio total energy calculations for metals and semiconductors using a plane-wave basis set, *Comput. Mater. Sci.* **6**, 15 (1996).
- [52] G. Kresse and J. Hafner, Ab initio molecular dynamics for liquid metals, *Phys. Rev. B* **47**, 558 (1993).
- [53] G. Kresse and J. Furthmüller, Efficient iterative schemes for ab initio total-energy calculations using a plane-wave basis set, *Phys. Rev. B* **54**, 11169 (1996).
- [54] J. P. Perdew, K. Burke, and M. Ernzerhof, Generalized gradient approximation made simple, *Phys. Rev. Lett.* **77**, 3865 (1996).
- [55] P. E. Blöchl, Projector augmented-wave method, *Phys. Rev. B* **50**, 17953 (1994).
- [56] G. Kresse and D. Joubert, From ultrasoft pseudopotentials to the projector augmented-wave method, *Phys. Rev. B* **59**, 1758 (1999).
- [57] V. I. Anisimov, J. Zaanen, and O. K. Andersen, Band theory and mott insulators: Hubbard U instead of stoner I, *Phys. Rev. B* **44**, 943 (1991).
- [58] S. L. Dudarev, G. A. Botton, S. Y. Savrasov, C. J. Humphreys, and A. P. Sutton, Electron-energy-loss spectra and the structural stability of nickel oxide: An LSDA+U study, *Phys. Rev. B* **57**, 1505 (1998).
- [59] M. Cococcioni and S. de Gironcoli, Linear response approach to the calculation of the effective interaction parameters in the LDA + U method, *Phys. Rev. B* **71**, 035105 (2005).
- [60] G. Pizzi, V. Vitale, R. Arita, S. Blügel, F. Freimuth, G. Géranton, M. Gibertini, D. Gresch, C. Johnson, T. Koretsune, J. Ibañez-Azpiroz, H. Lee, J.-M. Lihm, D. Marchand, A. Marrazzo, Y. Mokrousov, J. I. Mustafa, Y. Nohara, Y. Nomura, L. Paulatto, S. Poncé, T. Ponweiser, J. Qiao, F. Thöle, S. S. Tsirkin, M. Wierzbowska, N. Marzari, D. Vanderbilt, I. Souza, A. A. Mostofi, and J. R. Yates, Wannier90 as a community code: new features and applications, *J. Phys.: Condens.Matter* **32**, 165902 (2020).
- [61] N. Marzari and D. Vanderbilt, Maximally localized generalized wannier functions for composite energy bands, *Phys. Rev. B* **56**, 12847 (1997).
- [62] I. Souza, N. Marzari, and D. Vanderbilt, Maximally localized wannier functions for entangled energy bands, *Phys. Rev. B* **65**, 035109 (2001).
- [63] Q. Wu, S. Zhang, H.-F. Song, M. Troyer, and A. A. Soluyanov, Wanniertools : An open-source software package for novel topological materials, *Comput. Phys. Commun.* **224**, 405 (2018).
- [64] Y. Zhou, F. Xiong, X. Wan, and J. An, Hopf-link topological nodal-loop semimetals, *Phys. Rev. B* **97**, 155140 (2018).